

## Phase coexistence in the charge ordering transition in $\text{CaMn}_7\text{O}_{12}$

R Przeniosło<sup>1,2</sup>, I Sosnowska<sup>2</sup>, E Suard<sup>1</sup>, A Hewat<sup>1</sup> and A N Fitch<sup>3</sup>

<sup>1</sup> Institut Laue–Langevin, 6 rue Jules Horowitz, BP-156X 38 042 Grenoble Cedex 9, France

<sup>2</sup> Institute of Experimental Physics, Warsaw University, Hoza 69, PL-00 681 Warsaw, Poland

<sup>3</sup> European Synchrotron Radiation Facility, BP 220, 38 043 Grenoble, France

Received 8 March 2002

Published 30 May 2002

Online at [stacks.iop.org/JPhysCM/14/5747](http://stacks.iop.org/JPhysCM/14/5747)

### Abstract

The structural phase transition in  $\text{CaMn}_7\text{O}_{12}$  has been investigated by using high-resolution synchrotron and neutron powder diffraction. Both measurements show a phase coexistence phenomenon: between 409 and 448 K two different crystallographic phases coexist in the material. The first one is trigonal and it has a charge ordering (CO) of the  $\text{Mn}^{3+}$  and  $\text{Mn}^{4+}$  ions, while the second one is cubic and charge delocalized (CD). The volume fraction of the CD phase increases with temperature from zero at 400 K up to 100% about 460 K. Both phases have domains of at least 150 nm at each temperature in the PS region. A percolation scenario assuming a growth of the volume of the highly conducting CD regions at the expense of the volume of the insulating CO matrix is discussed and it is found to be in agreement with literature data of the  $\text{CaMn}_7\text{O}_{12}$  resistivity.

One of the most interesting phenomena observed in manganite perovskite systems is the so-called phase separation (PS) phenomenon described in a review paper by Dagotto *et al* [1]. The competition of the electronic and lattice degrees of freedom can lead to the formation of sub-micrometre regions with different crystallographic structures in the lattice. PS has been observed in several manganite oxides with experimental studies [2–5] and it has also been theoretically described [1]. In most cases, one phase is charge ordered (CO) with antiferromagnetic order and insulating, while the other is charge delocalized (CD) with ferromagnetic order and metallic conductivity. Large sub-micrometre regions of such phases co-exist in some temperature interval and the volume fraction of one phase increases/decreases at the expense of the other with changing temperature. The increase of the volume fraction of the conducting phase regions leads to a decrease of the resistivity, which has been successfully described with percolation theory by Uehara *et al* [2] in the case of  $\text{La}_{5/8-y}\text{Pr}_y\text{Ca}_{3/8}\text{MnO}_3$ . Another example of PS has been found in synchrotron radiation (SR) studies of the layered perovskite system  $\text{LaSr}_2\text{Mn}_2\text{O}_7$  by Argyriou *et al* [3] and neutron diffraction studies of  $\text{La}_{2-2x}\text{Sr}_{1+2x}\text{Mn}_2\text{O}_7$  ( $x = 0.8$ ) by Ling *et al* [4] and  $\text{Pr}_{0.7}\text{Ca}_{0.3}\text{MnO}_3$  by Radaelli *et al* [5].

**Table 1.** Positions of ions in  $\text{CaMn}_7\text{O}_{12}$  in the low-temperature CO trigonal phase (space group  $R\bar{3}$ —coordinates are given in the hexagonal setting) and in the high-temperature CD cubic phase (space group  $Im\bar{3}$ ). The symbols A, B and O refer to the sublattices in the perovskite structure  $\text{ABO}_3$ . The  $\text{Mn}^{3+}$  and  $\text{Mn}^{4+}$  ions of the B sublattice are separated in the (9d) and (3b) sites in the trigonal phase but they merge into one (8c), mixed-valence Mn site in the cubic phase. The  $\text{O}^{2-}$  ions in two different trigonal (18f) sites merge into one cubic (24g) site. The trigonal and cubic phases contain three and two  $\text{CaMn}_7\text{O}_{12}$  formula units in the unit cell, respectively.

Subl.	Ion	Pos. ( $R\bar{3}$ )	$x_h$	$y_h$	$z_h$	Pos. ( $Im\bar{3}$ )	$x_c$	$y_c$	$z_c$
A	$\text{Ca}^{2+}$	(3a)	0	0	0	(2a)	0	0	0
A	$\text{Mn}^{3+}$	(9e)	1/2	0	0	(6b)	1/2	1/2	0
B	$\text{Mn}^{3+}$	(9d)	1/2	1/2	1/2	(8c)	1/4	1/4	1/4
B	$\text{Mn}^{4+}$	(3b)	0	0	1/2	(8c)	1/4	1/4	1/4
O	$\text{O}^{2-}$	(18f)	$x_1$	$y_1$	$z_1$	(24g)	$x$	$y$	0
O	$\text{O}^{2-}$	(18f)	$x_2$	$y_2$	$z_2$	(24g)	$x$	$y$	0

There are also manganite systems where the two separated phases coexist down to the temperatures of about 2 K as shown by Frontera *et al* [6] in the case of  $\text{Bi}_{0.5}\text{Sr}_{0.5}\text{MnO}_3$ .

In this paper we present studies of the CO associated with a crystallographic phase transition from a CO phase to a CD phase in the manganite oxide system  $\text{CaMn}_7\text{O}_{12}$ . The transition occurs between 400 and 460 K, which is a relatively high temperature for manganite compounds. The CO temperature of 475 K observed by Garcia-Muñoz *et al* [7] in  $\text{Bi}_{1/2}\text{Sr}_{1/2}\text{MnO}_3$  was reported as *spectacularly high*. The crystal structure of  $\text{CaMn}_7\text{O}_{12}$  is trigonal (space group  $R\bar{3}$ ) at RT [8] and above 440 K it becomes cubic (space group  $Im\bar{3}$ ) [9]. The trigonal-to-cubic phase transition has been already studied by Troyanchuk and Chobot [9]. The ac and dc conductivity, the IR transmission at  $\mu = 800 \text{ cm}^{-1}$  and Young's modulus of  $\text{CaMn}_7\text{O}_{12}$  change in a jumpwise manner near 440 K. The x-ray diffraction measurements of Troyanchuk and Chobot [9] reported a large change of the pseudocubic<sup>4</sup> angle  $\alpha_c$  and a jumpwise change of the unit-cell volume at 440 K.

Neutron powder diffraction studies have shown that  $\text{CaMn}_7\text{O}_{12}$  has a complex modulated magnetic ordering, which shows a separation of two different magnetic phases [10–12], but above 90 K the system is paramagnetic.

The distribution of the ions among the crystallographic positions in both structures is described in table 1. The lattice constants of  $\text{CaMn}_7\text{O}_{12}$  at RT reported in [8] were  $a_h = 10.441 \text{ \AA}$  and  $c_h = 6.343 \text{ \AA}$  in the hexagonal setting of space group  $R\bar{3}$  (this hexagonal setting will be used in this paper). The crystal structure of  $\text{CaMn}_7\text{O}_{12}$  corresponds to a distortion of the perovskite structure  $\text{ABO}_3$ . The charge separation of  $\text{Mn}^{3+}$  and  $\text{Mn}^{4+}$  ions, proposed in [8], gives an electrostatically neutral unit cell with the ratio of numbers of  $\text{Mn}^{3+}$  to  $\text{Mn}^{4+}$  ions equal to 6:1. The  $\text{Mn}^{4+}$  ions in (3b) positions have a  $\bar{3}$  point symmetry with six oxygen neighbours at the same distance,  $1.911 \text{ \AA}$  [8]. The  $\text{Mn}^{3+}$  ions located in the (9d) positions have a Jahn–Teller apically contracted  $\text{MnO}_6$  octahedron with two pairs of long equatorial bonds,  $2.037 \text{ \AA}$  and  $2.041 \text{ \AA}$ , and one pair of short apical bonds of  $1.892 \text{ \AA}$  [8]. The  $\text{Mn}^{3+}$  ions located in (9e) positions are surrounded by 12 oxygen ions, which form a tetracapped rhombic prism with six sets of two equal Mn–O distances. The two shortest Mn–O bond lengths are  $1.912$  and  $1.906 \text{ \AA}$  for (9e) [8].

The important structural feature is that the topological network of nearest Mn–O bonds in  $\text{CaMn}_7\text{O}_{12}$  is different as compared with other manganite systems with distorted perovskite

<sup>4</sup> The pseudocubic angle  $\alpha_c$ , referred to in [9] as  $\alpha$ , is most probably the angle between two Ca–Mn axes, which is equal to  $90^\circ$  in the cubic phase and about  $90.33^\circ$  in the trigonal phase.  $\alpha_c$  is not the rhombohedral angle  $\alpha$ , which is equal to about  $109.6^\circ$  in  $\text{CaMn}_7\text{O}_{12}$  at RT [8].

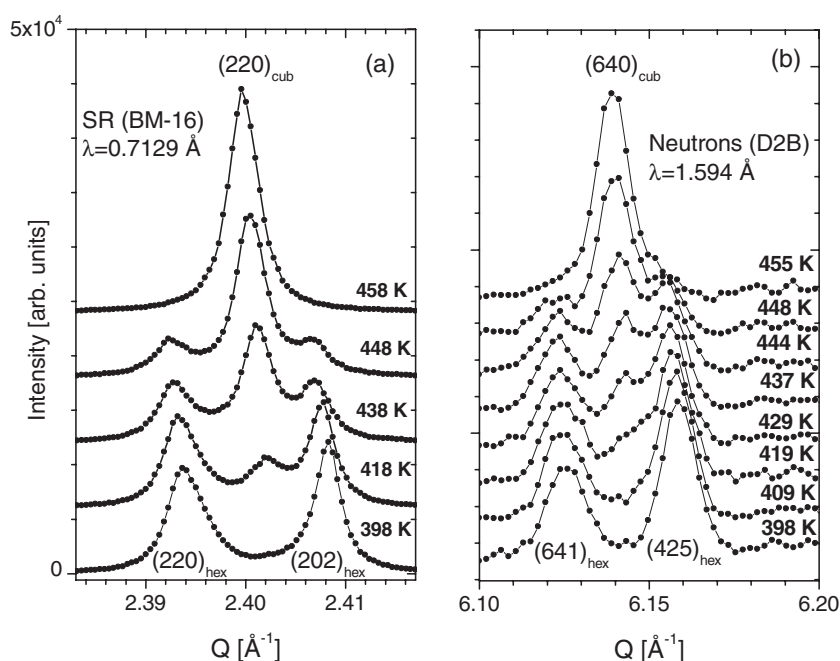


**Figure 1.** Representative parts of the SR (a) and neutron (b) powder diffraction patterns of  $\text{CaMn}_7\text{O}_{12}$  measured in the PS region. Solid circles represent measured data and the curves are shown to guide the eye.  $Q$  is the length of the scattering vector calculated as  $Q = (4\pi/\lambda) \sin \theta$ , where the scattering angle is  $2\theta$ . The patterns measured at different temperatures are vertically shifted for clarity.

structure such as  $\text{La}_x\text{Ca}_{1-x}\text{MnO}_3$  [13] or more general Ruddlesen–Popper phases [14, 15]. In these systems the oxygen ions form tilted and/or distorted corner sharing octahedra, so every oxygen ion has two nearest-neighbour Mn ions. In the low-temperature trigonal and high-temperature cubic structures of  $\text{CaMn}_7\text{O}_{12}$  every oxygen ion *has not two, but three nearest-neighbour Mn ions*. Within the structural model of  $\text{CaMn}_7\text{O}_{12}$  [8] every oxygen atom in the O1 sublattice has three Mn ions at 2.037, 1.912 and 1.892 Å, and the same for the O2 sublattice, with three Mn atoms at 2.041, 1.911 and 1.906 Å.

The SR diffraction measurements of  $\text{CaMn}_7\text{O}_{12}$  have been performed with a wavelength of 0.710 29 Å at the BM-16 beamline, ESRF Grenoble for temperatures from RT up to 460 K. The polycrystalline sample was mounted in a 0.3 mm diameter capillary. The neutron powder diffraction measurements have been performed at the high-resolution diffractometer D2B, ILL Grenoble, operating at a wavelength of 1.594 Å with a 10' primary beam collimation, for temperatures between 400 and 455 K. The polycrystalline sample was mounted in a 15 mm diameter vanadium container. The data acquisition time for every SR and neutron diffraction pattern was 1 and 2.5 h, respectively. During these measurements the temperature stability of the sample was better than 0.2 K.

Representative parts of the SR and neutron diffraction patterns are shown in figures 1(a) and (b) respectively. One can see that the peaks due to both the trigonal and cubic phases coexist in a large temperature interval between 418 and 448 K. The Bragg peaks due to the two phases are clearly separated and from the FWHM of the SR diffraction peaks one can estimate that the correlation length of both phases is at least 150 nm.

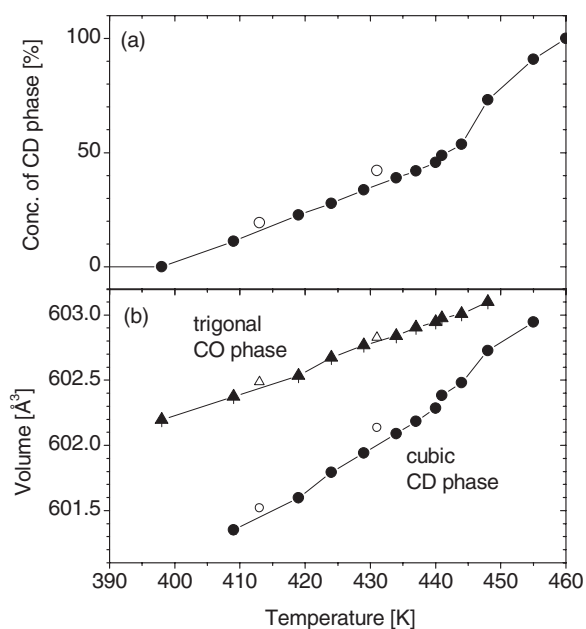


**Figure 2.** Temperature dependence of the CD phase concentration (a), the unit-cell volume of the trigonal CO phase (triangles) (b) and the unit-cell volume (multiplied by 1.5) of the cubic CD phase (circles) (b). All these values are determined from Rietveld analysis of powder neutron diffraction data of  $\text{CaMn}_7\text{O}_{12}$ . The full symbols show values measured with warming between the temperature steps, the open symbols those measured with cooling.

The neutron diffraction patterns were analysed with the Rietveld method and the program FullProf [16], assuming two phases of  $\text{CaMn}_7\text{O}_{12}$ : the low-temperature CO trigonal phase as described by Bochu *et al* [8] and the high-temperature CD cubic phase similar to the structure of  $\text{CaCu}_3\text{Mn}_4\text{O}_{12}$  [17]. There was one spurious reflection in the neutron diffraction patterns near  $Q = 7.58 \text{ \AA}^{-1}$  due to the scattering on the Al tail of the cryofurnace. This peak was excluded from the refinements. There were also two small impurity phases found:  $\text{Mn}_2\text{O}_3$  (2.2 vol.%) and  $\text{Mn}_3\text{O}_4$  (2.5 vol.%), in agreement with earlier neutron diffraction measurements on the same polycrystalline sample [11]. The Bragg factor  $R_B$  for both phases varied between 4.8 and 5.8%; the  $\chi^2$  factor varied between 2.9 and 4.4%. The volume concentration of the CD phase, defined as the total volume of the CD phase divided by the sum of the volumes of both CO and CD phases, is shown in figure 2(a). The concentration of the CD phase first increases linearly with temperature up to 440 K, and then starts to grow faster. This result should be compared with literature data on the resistivity of  $\text{CaMn}_7\text{O}_{12}$  [9, 18], which show a sharp decrease of one order of magnitude between 440 and 450 K. The concentration of the CD phase at 440 K is equal to 48(2)% and the behaviour of the resistivity can be qualitatively explained in terms of the percolation theory. Between 400 and 440 K the CO phase melts and large regions of the CD phase start to grow, but their concentration is small and the resistivity of the system remains large. Above 440 K the concentration goes beyond the value of  $c = 0.5$  and the resistivity of the system decreases considerably. It should be mentioned that the percolation threshold [19] for a three-dimensional system is usually found for concentrations between 25 and 33%. The threshold observed in the present study is about 48%, so a simple model of site or bond percolation seems not to be appropriate. Further data analysis will show that the metric properties of the CO phase change at the same concentration threshold of about 48%.

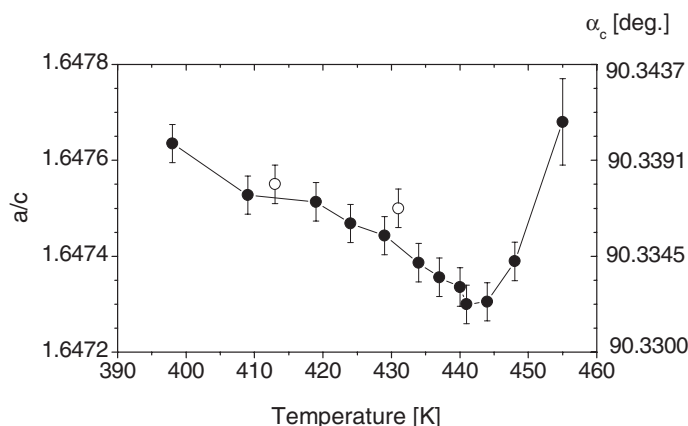


**Figure 3.** Temperature dependence of the  $a/c$  lattice parameter ratio in the CO trigonal phase of  $\text{CaMn}_7\text{O}_{12}$  determined from neutron powder diffraction data. The right-hand scale shows the corresponding values of the angle between the pseudo-cubic axes (see text). The full symbols show values measured on warming while the open symbols those on cooling.

The unit-cell volumes of both phases are shown in figure 2(b) and one can see that the unit-cell volume of the insulating CO phase is larger than the corresponding unit-cell volume of the conducting CD phase by about 0.16% at 409 K and 0.08% at 448 K. X-ray studies by Troyanchuk and Chobot [9] reported a volume increase of the volume of unit cell by 0.11% on passing from the trigonal to the cubic phase in disagreement with present results (figure 2(b)). The results of this paper agree with studies of other manganite compounds [3, 5] where the volume of the unit cell of the CO phase was larger than the CD phase. The concentration of the CD phase (figure 2(a)) as well as the unit-cell volumes (figure 2(b)) and the trigonal distortion (figure 3) determined by warming and cooling are slightly different, which shows that the transition is of first order with a weak hysteresis of a few kelvins.

It is interesting to note that the structural properties of the trigonal CO phases only slightly change with temperature. The ratio of the trigonal lattice parameters  $a/c$  is shown in figure 3. The right-hand scale denotes the corresponding values of the pseudocubic angle  $\alpha_c$ , which can be calculated from

$$\cos \alpha_c = \frac{1 - \frac{3}{8}(a/c)^2}{1 + \frac{3}{4}(a/c)^2}.$$

The  $a/c$  ratio has a minimum about 440 K, i.e. when the concentration of the CD phase becomes larger than 50%. This implies that the structural properties of the CO phase start to change when the CO becomes a minority phase. One should however note that the change of the pseudocubic angle is of the order of only  $0.01^\circ$ . This is in contrast with x-ray diffraction studies of  $\text{CaMn}_7\text{O}_{12}$  by Troyanchuk and Chobot [9], who reported a change of  $\alpha_c$  of about  $0.2^\circ$ .

The most physically significant difference between the structural properties of both CO and CD phases is related to different Mn–O bond lengths. The Jahn–Teller  $\text{Mn}^{3+}$  ions in (9d) positions (CO phase) have distorted  $\text{MnO}_6$  octahedra, while the CD Mn ions in (24g) positions (CD phase) have undistorted  $\text{MnO}_6$  octahedra. The temperature dependences of the length of the Mn–O bonds for the various Mn ions located in the B-type sublattice are shown in figure 4. One can see that the Mn–O bond lengths do not change considerably in the PS region. The strong Jahn–Teller distortion of the  $\text{MnO}_6$  octahedra around the  $\text{Mn}^{3+}$  ions in (9d) positions in the CO phase also does not change with temperature.

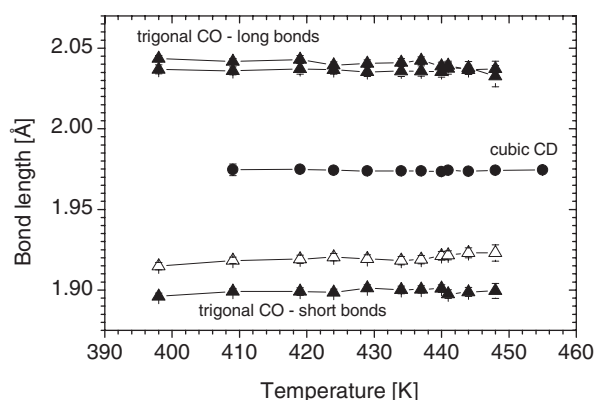


**Figure 4.** Length of the Mn–O bonds for Mn ions located in the B sublattice of  $\text{CaMn}_7\text{O}_{12}$ . The Jahn–Teller-distorted  $\text{Mn}^{3+}$  in (9d) trigonal (CO) sites have three different Mn–O bondlengths (solid triangles) and the undistorted  $\text{Mn}^{4+}$  in (3b) trigonal (CO) sites have one Mn–O bondlength (open triangles). The corresponding Mn ions in the CD cubic phase located in (8c) sites have one bondlength (circles).

The present studies clearly show that the electronic properties of the Mn ions in the two phases are different. It can be concluded that it is energetically favourable to maintain large clusters of CD phase growing in a matrix of melting CO phase rather than to continuously change from CO to CD structure. The separation of phases with different densities in  $\text{R}_{1-x}\text{A}_x\text{MnO}_3$  (R—rare earth ion, A—alkaline ion) manganites was discussed by Dagotto *et al* [1]; however, their theoretical considerations predicted only small, nanometre-size clusters. The present case of  $\text{CaMn}_7\text{O}_{12}$  is structurally different because the  $\text{Ca}^{2+}$  and  $\text{Mn}^{3+}$  ions occupy different crystallographic positions in the A sublattice and they do not form a solid solution as in  $\text{R}_{1-x}\text{A}_x\text{MnO}_3$  manganite systems. The present results are more similar to the phase segregation in  $\text{Pr}_{0.7}\text{Ca}_{0.3}\text{MnO}_3$  [5], where the densities of the CO and CD phases differ by about 0.2%. On the other hand, the PS observed by Frontera *et al* [6] in  $\text{Bi}_{0.5}\text{Sr}_{0.5}\text{MnO}_3$  showed much larger density difference of about 1%.

Finally, it should also be pointed out that a coexistence of two different crystallographic phases has been found in SR diffraction studies of  $\text{LiMn}_2\text{O}_4$  by Massarotti *et al* [20]. According to [20] two cubic and orthorhombic phases coexist between 291.6 and 285 K on cooling and between 305 and 320 K on warming. The transition in  $\text{LiMn}_2\text{O}_4$  also occurs in the paramagnetic phase, similar to the present results for  $\text{CaMn}_7\text{O}_{12}$ . The difference is that not such a large temperature hysteresis was observed in  $\text{CaMn}_7\text{O}_{12}$ .

### Acknowledgments

Thanks are due to F Thomas for help with the sample environment equipment. This research was supported through a European Community Marie Curie Fellowship (RP). This work was partially supported by the Committee for Scientific Research (Poland).

### References

- [1] Dagotto E, Hotta T and Moreo A 2001 *Phys. Rep.* **344** 1
- [2] Uehara M, Mori S, Chen C H and Cheong S-W 1999 *Nature* **399** 560
- [3] Argyriou D N *et al* 2000 *Phys. Rev. B* **61** 15 269

- [4] Ling C D, Millburn J E, Mitchell J F, Argyriou D N, Linton J and Bordallo H N 2000 *Phys. Rev.* **62** 15 096
- [5] Radaelli P G, Ibberson R M, Argyriou D N, Casalta H, Andersen K H, Cheong S-W and Mitchell J F 2001 *Phys. Rev. B* **63** 172419
- [6] Frontera C, Garcia-Muñoz J L, Aranda M A G, Ritter C, Respaud M and Vanacken J 2001 *Phys. Rev. B* **64** 054401
- [7] Garcia-Muñoz J L, Frontera, Aranda M A G, Llobet A and Ritter C 2001 *Phys. Rev. B* **63** 064415
- [8] Bochu B, Buevoz J L, Chenavas J, Collomb A, Joubert J C and Marezio M 1980 *Solid State Commun.* **36** 133
- [9] Troyanchuk I O and Chobot A N 1997 *Crystallogr. Rep.* **42** 983
- [10] Przeniosło R, Sosnowska I, Żótek M, Hohlwein D and Troyanchuk I O 1998 *Physica B* **241–3** 730
- [11] Przeniosło R, Sosnowska I, Hohlwein D, Hauß T and Troyanchuk I O 1999 *Solid State Commun.* **111** 687
- [12] Przeniosło R, Sosnowska I, Strunz P, Hohlwein D, Hauß T and Troyanchuk I O 2000 *Physica B* **276–278** 547
- [13] Wollan E O and Koehler W C 1955 *Phys. Rev.* **100** 545
- [14] Ruddlesden S N and Popper D 1951 *Acta Crystallogr.* **10** 538
- [15] Fawcett I D, Sunstrom J E, Greenblatt M, Croft M and Ramanujachary K V 1998 *Chem. Mater.* **10** 3643
- [16] Rodríguez-Carvajal J 1992 *Physica B* **192** 55
- [17] Chenavas J, Joubert J C, Marezio M and Bochu B 1975 *J. Solid State Chem.* **14** 25
- [18] Troyanchuk I O, Lobanovsky L S, Kasper N V, Hervieu M, Maignan A, Michel C, Szymczak H and Szewczyk A 1998 *Phys. Rev. B* **58** 14 903
- [19] Stauffer D and Aharony A 1994 *Introduction to Percolation Theory* (London: Taylor and Francis)
- [20] Massarotti V, Capsoni D, Bini M, Scardi P, Leoni M, Baron V and Berg H 1999 *J. Appl. Crystallogr.* **32** 1186